

# Tapered quantum cascade lasers operating at $9.0\ \mu\text{m}^*$

Gao Yu(高瑜), Liu Fengqi(刘峰奇)<sup>†</sup>, Liu Junqi(刘俊岐), Li Lu(李路), Wang Lijun(王利军),  
and Wang Zhanguo(王占国)

(Key Laboratory of Semiconductor Materials Science, Institute of Semiconductors, Chinese Academy of Sciences, Beijing 100083, China)

**Abstract:** The tapered quantum cascade lasers operating at about  $9.0\ \mu\text{m}$  are reported. In contrast to the common ridge waveguide laser, tapered devices give rather small horizontal beam divergence. Performances of devices with identical  $11\ \mu\text{m}$  ridge waveguide sections and different tapered gain sections are comparatively studied. The optimal taper angle of  $3^\circ$  leads to a relative high output power and a very small horizontal beam divergence of  $7.1^\circ$ .

**Key words:** quantum cascade lasers; InGaAs/InAlAs/InP; tapered;  $9.0\ \mu\text{m}$

**DOI:** 10.1088/1674-4926/31/3/034008

**PACC:** 4260D; 7850G

## 1. Introduction

Quantum cascade lasers (QCLs)<sup>[1]</sup> are unipolar semiconductor devices based on intersubband transitions between quantized subband states in a multiple quantum well heterostructure. Since their invention in 1994<sup>[2]</sup>, the performance of QCLs has been improved dramatically by optimizing the material quality and processing technology. Now QCLs are capable of covering the wavelength range of  $3\text{--}25\ \mu\text{m}$ , which makes them a very desirable source for technological applications such as gas sensing, industrial process monitoring and space communication. However, the divergence of the laser beam limits the resolution and efficiency of the QCLs in almost all of their applications<sup>[3,4]</sup>.

Ridge waveguide tapered lasers consisting of a ridge waveguide section and a tapered gain section are promising structures for narrow horizontal beam divergence at high output power. For conventional quantum well lasers, the tapered structures have been extensively studied and nearly diffraction limited beam qualities have been obtained<sup>[5–9]</sup>. For QCLs, however, reports about the application of the tapered structures are very few<sup>[10,11]</sup>. What is more, the related studies are far from enough for guiding the design of tapered QCLs. For example, though the horizontal beam divergence was reported to decrease with the increase of the taper angle<sup>[10]</sup>, the dependence of output power on the angle was not studied.

In this paper, we report the systematic optimization of the structure of  $9.0\ \mu\text{m}$  tapered quantum cascade lasers. Devices with different taper angles are presented. With the increase of taper angle, a small horizontal beam divergence about  $7.1^\circ$  is realized. For a specific  $11\ \mu\text{m}$  ridge waveguide section, optimal taper angle leads to a relative high output power combined with a very small horizontal beam divergence.

## 2. Fabrication and measurement

The quantum cascade laser structure demonstrated in this

paper was grown on an n-doped ( $\text{Si}, 3 \times 10^{17}\ \text{cm}^{-3}$ ) InP substrate by solid-source molecular beam epitaxy (MBE) in a single growth step. The active region, which consists of 35-period lattice matched  $\text{In}_{0.53}\text{Ga}_{0.47}\text{As}/\text{In}_{0.52}\text{Al}_{0.48}\text{As}$  wells and barriers layers of superlattice, is based on a four quantum well double phonon resonance design<sup>[12]</sup>. The active region is sandwiched between a  $0.4\text{-}\mu\text{m}$ -thick below and a  $0.5\text{-}\mu\text{m}$ -thick upper Si-doped ( $6 \times 10^{16}\ \text{cm}^{-3}$ )  $\text{In}_{0.53}\text{Ga}_{0.47}\text{As}$  below layers. The upper cladding layer consists of a  $2\text{-}\mu\text{m}$ -thick InP layer doped with Si ( $n = 1 \times 10^{17}\text{--}3 \times 10^{17}\ \text{cm}^{-3}$ ). The growth ended with a  $0.5\text{-}\mu\text{m}$ -thick heavily Si-doped ( $6 \times 10^{18}\ \text{cm}^{-3}$ ) InP layer.

The schematic structure of the tapered QCLs is shown in Fig. 1. The tapered laser consists of a ridge waveguide (RW) section coupled to a tapered section. The width of the RW section in this work is about  $11\ \mu\text{m}$ . The taper angles of the QCLs studied in this work are  $1^\circ, 2^\circ, 3^\circ$  and  $4^\circ$  respectively. The tapered QCLs are deeply etched through the whole active region to form index guided tapered sections. The tapered quantum cascade laser structures are defined on the wafer by the conventional photolithography, then the wafer was deeply

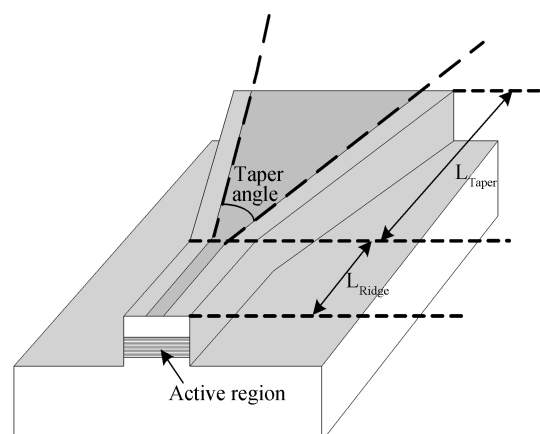


Fig. 1. Schematic picture of a tapered QCL.

\* Project supported by the National Science Fund for Distinguished Young Scholars (No. 60525406), the National Natural Science Foundation of China (Nos. 60736031, 60806018, 60906026), the National Basic Research Program of China (No. 2006CB604903), and the National High-Tech R&D Program of China (Nos. 2007AA03Z446, 2009AA03Z403).

<sup>†</sup> Corresponding author. Email: fqliu@semi.ac.cn

Received 8 September 2009, revised manuscript received 8 October 2009

© 2010 Chinese Institute of Electronics

etched to the substrate with a nonselective HBr : HNO<sub>3</sub> : H<sub>2</sub>O = 1 : 1 : 10 solution. A 350-nm-thick SiO<sub>2</sub> layer was deposited by chemical vapor deposition for electrical insulation around the pattern. For current injection, windows were opened on top of the ridge section and the taper section. Nonalloyed Ti/Au ohmic contacts were provided to the top layer. After the wafer was thinned to about 100 μm, the bottom Ti/Au contacts were formed. Lasers were cleaved manually with the facets uncoated, soldered epilayer-down onto Cu heat sinks and finally wire bonded.

For characterization, the lasers were mounted into a liquid nitrogen cooled cryostat. The optical output power emitted from the front facet of the laser was measured with a thermopile detector placed directly near the window of the cryostat. The output power is not corrected by the transmission of the optics windows (BaF<sub>2</sub>, the transmission efficiency is about 92% for the wavelength about 9 μm) and the collection efficiency of the detector. (The collection efficiency is limited by the distance between cryostat and detector, and the far-field distribution of the laser. The estimated value is about 60%)<sup>[13]</sup>. For far-field characterization, the cryostat was fixed on a rotation stage. A nitrogen-cooled HgCdTe detector was located 10-cm distance away to collect the lasing light.

### 3. Device performance

Figure 2(a) shows the light output–current ( $L-I$ ) curves of the tapered QCLs with varied taper angles measured at 85 K. The length of both the tapered section (LT) and the RW section (LR) are 1mm. For comparison, the  $L-I$  curve of a 2-mm long RW QCL is also shown in the figure. The curves were measured under pulse conditions with a repetition rate of 1 kHz and a pulse width of 1 μs. As can be seen from Fig. 2(a), the peak output power of the tapered QCLs is much larger than that of the RW QCLs. What is more, the peak output power increased continuously when the taper angles increase from 1° to 3° and then dropped suddenly when the taper angle increase further to 4°. Similar trends have also been found for other groups of tapered QCLs with different LT/LR. Figure 2(b) shows the ratios of the peak output powers and the volumes of the gain material (area) of the tapered lasers to those of the RW laser as a function of the taper angles. Hereafter, the taper angle of the RW QCLs is designated as 0°. As can be seen from the figure, the larger peak output power of the tapered QCLs is related to the larger volume of the gain material. The peak output power increases with the volume of the gain material for the QCLs with taper angles smaller than 3°. What is more, the increase of the output power is noticeably larger than that of the gain material. This might result from the more efficient waveguiding of the optical mode in the tapered section<sup>[10, 14]</sup>. For the QCLs with 4° taper angle, however, the power ratio of the tapered laser to the RW laser is 1.7 which is smaller than the increase ratio of the gain material (2.56). This drop of output power can be attributed to the strong thermal accumulation resulted from the large volume of gain sections of the 4° tapered QCLs<sup>[15]</sup>, which counteracts the amplification effect of the taper section. Figure 3 shows the threshold current density of the tapered QCLs as a function of the taper angle. As can be seen, the threshold current densities of the tapered QCLs are higher than that of the RW QCL. This has resulted in the loss caused by the reflected radiation cou-

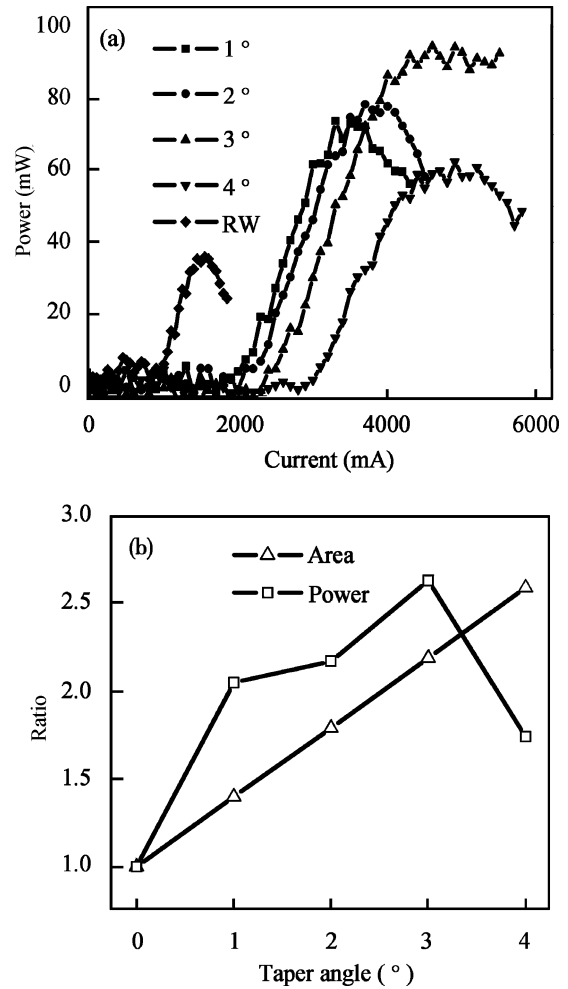


Fig. 2. (a) Pulsed  $L-I$  curves at 85 K of the 2-mm-long RW and tapered QCLs (Taper angles: 1°, 2°, 3° and 4°). (b) Ratio of the peak output power and the volumes of the gain material of the tapered lasers to the RW lasers versus taper angle (defining the taper angle for the RW QC laser is 0°).

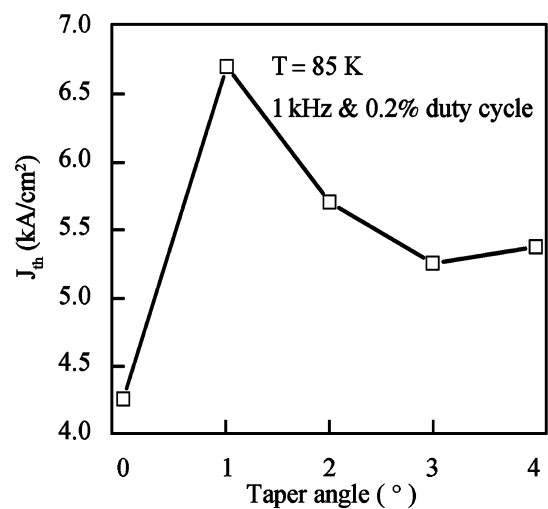


Fig. 3. Threshold current density of the tapered QCL versus the taper angle (defining the taper angle of the RW QC laser is 0°).

pled into the ridge waveguide section<sup>[6, 16]</sup>. The above results show that the optimized taper angle is 3° as far as the peak

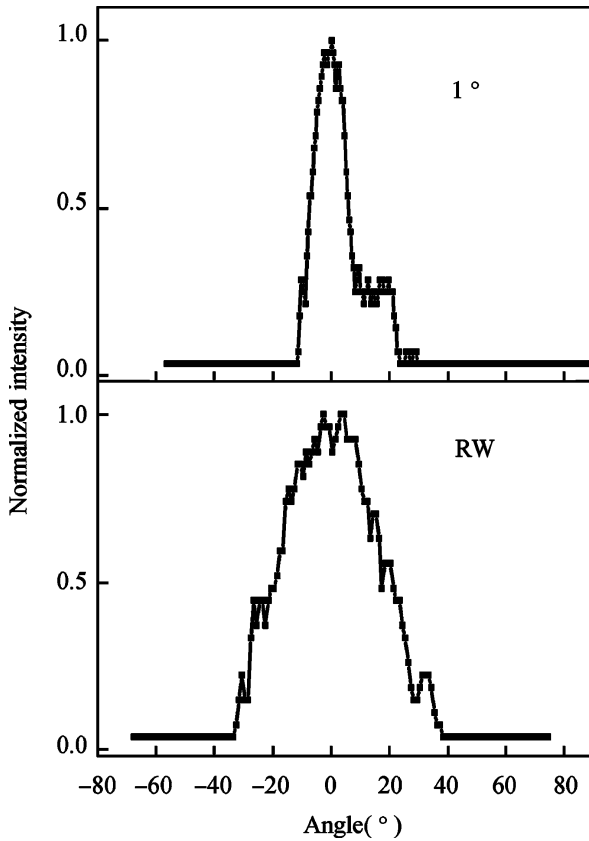


Fig. 4. Measured horizontal far-field intensity profiles of the RW QCLs and the tapered QCLs with the taper angle of 1°.

output power of the lasers is concerned.

The measured horizontal far-field profiles of the RW QCL and the tapered QCL with a taper angle of 1° are shown in Fig. 4. The curves are measured at 85 K under pulse conditions with the pulse duration and repetition rate being 2 μs and 1 kHz, respectively. The RW QCL is 2 mm long and the tapered QCL is about 4 mm long with a 1.5-mm long RW section and a 2.5-mm tapered section. As shown in the figure, the full width at half maximum (FWHM) of the tapered QCL is only 13.4°, whereas the FWHM of the RW QCL is as large as 39.1°. Figure 4 shows that by introducing a tapered section, the QCLs can have a significantly smaller beam divergence than the RW QCLs, which is desirable for their applications.

By varying the taper angles of the QCLs the horizontal far field angle of the devices can be further improved. Figure 5(a) shows the typical experimental horizontal far-field profiles of the tapered QCLs with varied taper angles. The measurement conditions and the structure of the tapered QCLs are the same as those of the tapered device shown in Fig. 4. As is shown in Fig. 5(b), the FWHM are 13.4°, 11.3°, 7.2° and 7.1° for the tapered QCLs with the taper angles of 1°, 2°, 3° and 4°, respectively. It is clear that the FWHM of the horizontal far-field profile decreases with the increase of the taper angles, however, at a slower rate for larger taper angles. As can be seen from Fig. 5(b), compared to the QCL with a taper angle of 3°, the FWHM of the 4° tapered QCL is narrowed only by 0.1°. Considering that the peak output power of the 4° tapered QCL is a lot smaller than that of the 3° tapered device, the optimal taper angle for the tapered QCL with an 11 μm width RW section is 3°.

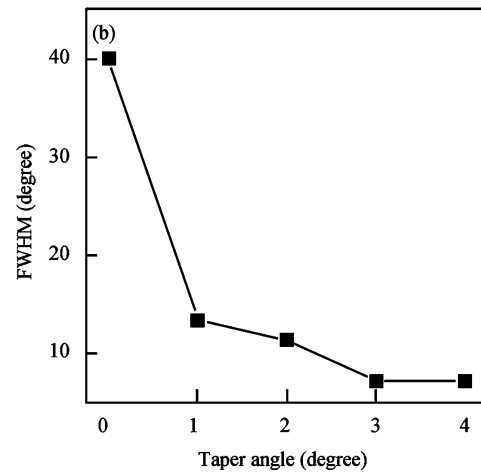
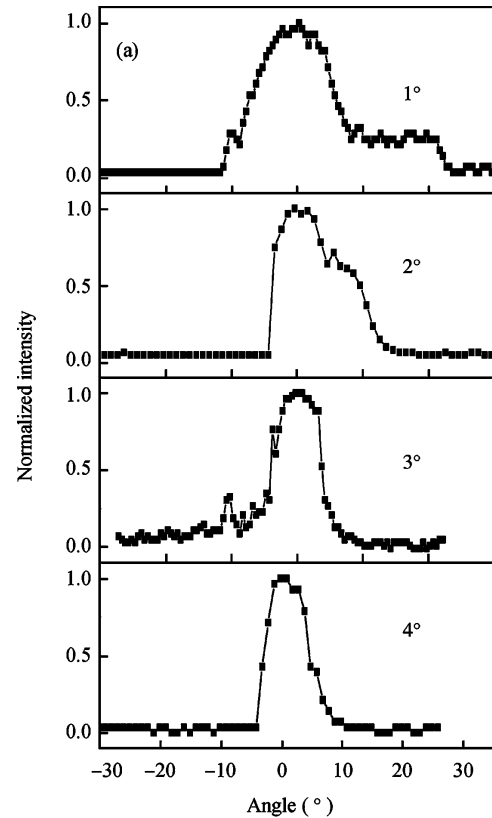


Fig. 5. (a) Measured horizontal far-field intensity profiles of the tapered QCLs with varied taper angles. (b) FWHM angle of the tapered QCL versus the taper angle.

### 4. Conclusion

In conclusion, the tapered QCLs emitting at the wavelength of about 9.0 μm are fabricated. The output character and the horizontal far-field profile of the tapered lasers are compared with the RW QCLs. By introducing the tapered section, a much narrower horizontal far-field FWHM angle is obtained. A larger taper angle brings to a narrower horizontal far-field FWHM. With the increase of the taper angle, the output power increase first, and then decrease suddenly. Taking both the output power and the horizontal far-field FWHM angle into account, 3° is the optimal taper angle for the tapered QCL emitting at the wavelength of about 9.0 μm with the ridge width of

about 11  $\mu\text{m}$ .

## Acknowledgements

The authors would like to acknowledge Liang Ping, Hu Ying, and Sun Hong for their help with device fabrication.

## References

- [1] Gmachl C, Capasso F, Sivco D L, et al. Recent progress in quantum cascade lasers and applications. *Rep Prog Phys*, 2001, 64: 1533
- [2] Faist J, Capasso F, Sivco D L, et al. Quantum cascade laser. *Science*, 1994, 264: 553
- [3] Li L, Liu F Q, Shao Y, et al. Low-threshold high-temperature operation of  $\lambda \sim 7.4 \mu\text{m}$  quantum cascade lasers. *Chin Phys Lett*, 2007, 24(6): 1577
- [4] Gresch T, Giovannini M, Hoyer N, et al. Quantum cascade lasers with large optical waveguides. *IEEE Photonics Technol Lett*, 2006, 18(3): 544
- [5] Li J, Ma X Y, Liu Y Y. High-power ridge-waveguide tapered diode lasers at 980 nm. *Chinese Journal of Semiconductors*, 2007, 28(5): 645
- [6] Walpole J N, Kintzer E S, Chinn S R, et al. High-power strained-layer InGaAs/AlGaAs tapered traveling wave amplifier. *Appl Phys Lett*, 1992, 61(7): 740
- [7] Kintzer E S, Walpole J N, Chinn S R, et al. High-power, strained-layer amplifiers and lasers with tapered gain regions. *IEEE Photonics Technol Lett*, 1993, 5(6): 605
- [8] Dittmar F, Sumpf B, Fricke J, et al. High-power 808-nm tapered diode lasers with nearly diffraction-limited beam quality of  $M^2 = 1.9$  at  $P = 4.4 \text{ W}$ . *IEEE Photonics Technol Lett*, 2006, 18(4): 601
- [9] Auzanneau S C, Calligaro M, Krakowski M. High brightness GaInAs/(Al)GaAs quantum-dot tapered lasers at 980 nm with high wavelength stability. *Appl Phys Lett*, 2004, 84(13): 2238
- [10] Nähle L, Semmel J, Kaiser W, et al. Tapered quantum cascade lasers. *Appl Phys Lett*, 2007, 91: 181122
- [11] Troccoli M, Gmachl C, Capasso F, et al. Mid-infrared ( $\lambda \approx 7.4 \mu\text{m}$ ) quantum cascade laser amplifier for high power single-mode emission and improved beam quality. *Appl Phys Lett*, 2002, 80(22): 4103
- [12] Darvish S R, Zhang W, Evans A, et al. High-power, continuous-wave operation of distributed-feedback quantum-cascade lasers at  $\lambda \sim 7.8 \mu\text{m}$ . *Appl Phys Lett*, 2006, 89: 251119
- [13] Liu J Q, Liu F Q, Lu X Z, et al. Realization of GaAs/AlGaAs quantum-cascade lasers with high average optical power. *Solid-State Electron*, 2005, 49: 1961
- [14] Walpole J N. Semiconductor amplifiers and lasers with tapered gain regions. *Opt Quantum Electron*, 1996, 28: 623
- [15] Slivken S, Yu J S, Evans A, et al. Ridge-width dependence on high-temperature continuous-wave quantum-cascade laser operation. *IEEE Photonics Technol Lett*, 2004, 16(3): 744
- [16] Delépine S, Gérard F, Pinquier A, et al. How to launch 1 W into single-mode fiber from a single 1.48- $\mu\text{m}$  flared resonator. *IEEE J Sel Topics Quantum Electron*, 2001, 7: 111